

---

# 1 Shape Optimization of a Photo Gun

---

## 1.1 Geometry

---

- latest geometry in Figure 1
- corresponding electric field for  $p = 3$ ,  $n_{\text{sub}} = 16$ ,  $V_{\text{el}} = -300$  kV and  $V_{\text{ar}} = 1$  kV
- (patches 32 . . . 35 are not entirely correct, missing the correct high voltage adapter)

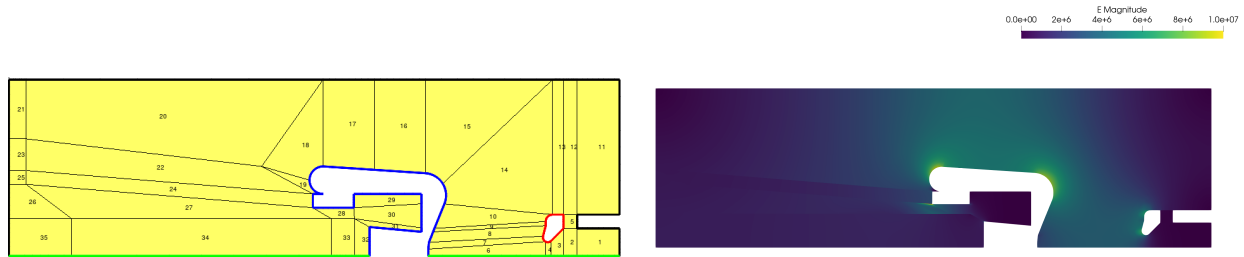


Figure 1: Initial geometry and magnitude of electric field.

---

## 1.2 Optimization

---

- optimized geometry in Figure 2
- cost function only takes into account electric field
- only the upper electrode shape is optimized (volume constraint could be kept as before at  $625 \text{ cm}^3$ )
- corresponding electric field for  $p = 3$ ,  $n_{\text{sub}} = 16$ ,  $V_{\text{el}} = -300$  kV and  $V_{\text{ar}} = 1$  kV
- **magnitude of E-field remains large in patch 14** (also around anode ring)

	$(V_{\text{el}} - 625)/\text{cm}^3$	$\max(\ \mathbf{E}\ _2)/\frac{\text{MV}}{\text{m}}$
• results:		
initial	2.445	9.295
optimized	-12.872	8.49



Figure 2: Optimized geometry and electric field.

### 1.3 Tracking

- **general settings:**  $Q = 100$  fC
- **spatial distribution:** Gaussian with  $\sigma = 400$   $\mu\text{m}$ , see Figure 3 for comparison with laser measurement (probe particles at  $0.5\sigma$ ,  $\sigma$ ,  $1.5\sigma$  in red)
- **temporal distribution:** Gaussian with  $\sigma = 5$  ps, see Figure 4 for comparison with measurement/model from [1]

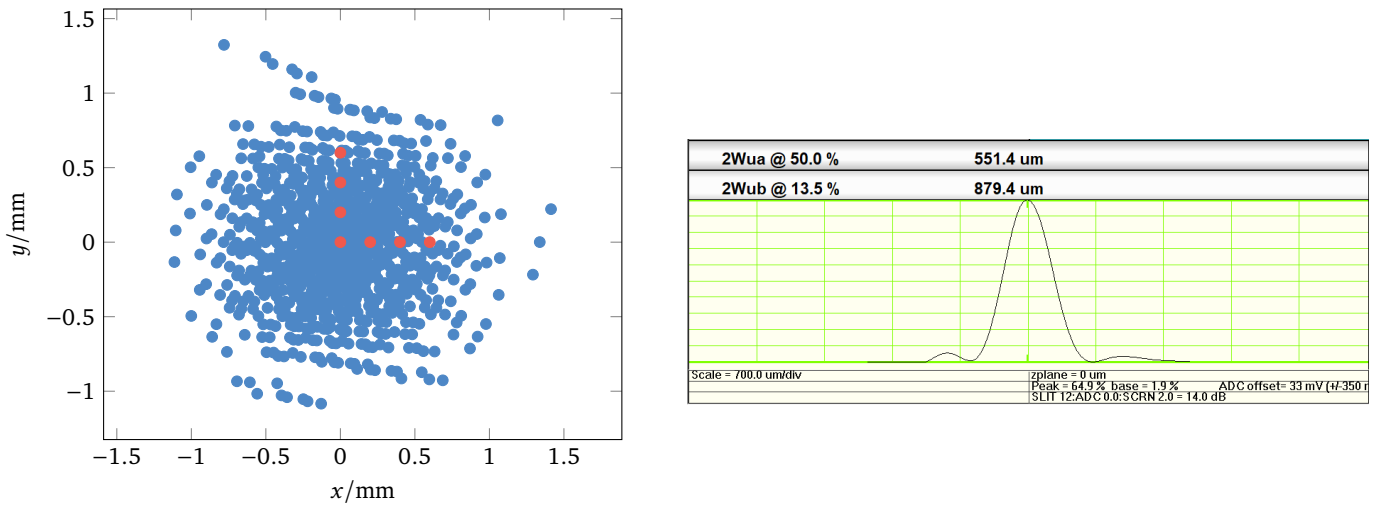


Figure 3: Spatial distribution ( $2^{10}$  particles) and laser measurement.

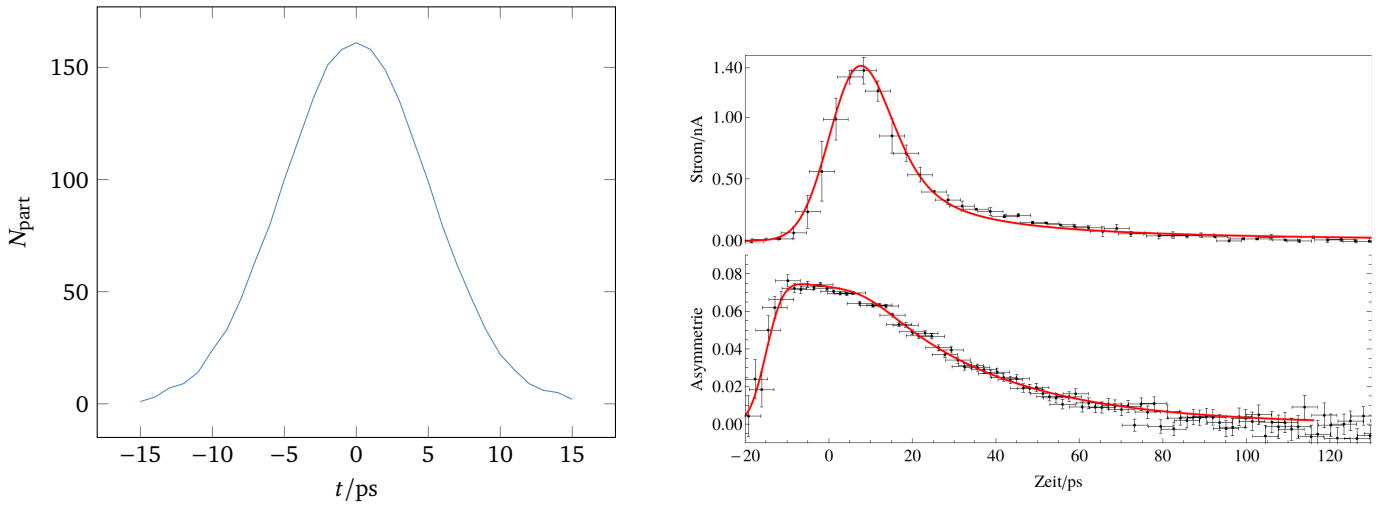


Figure 4: Temporal distribution ( $2^{10}$  particles) and measurement/model.

- **convergence of time integrator:** difference of normalized transverse emittance  $\epsilon$  w. r. t. finest time step is shown in Figure 5
- $H = 2^{-11}$  ns used later on

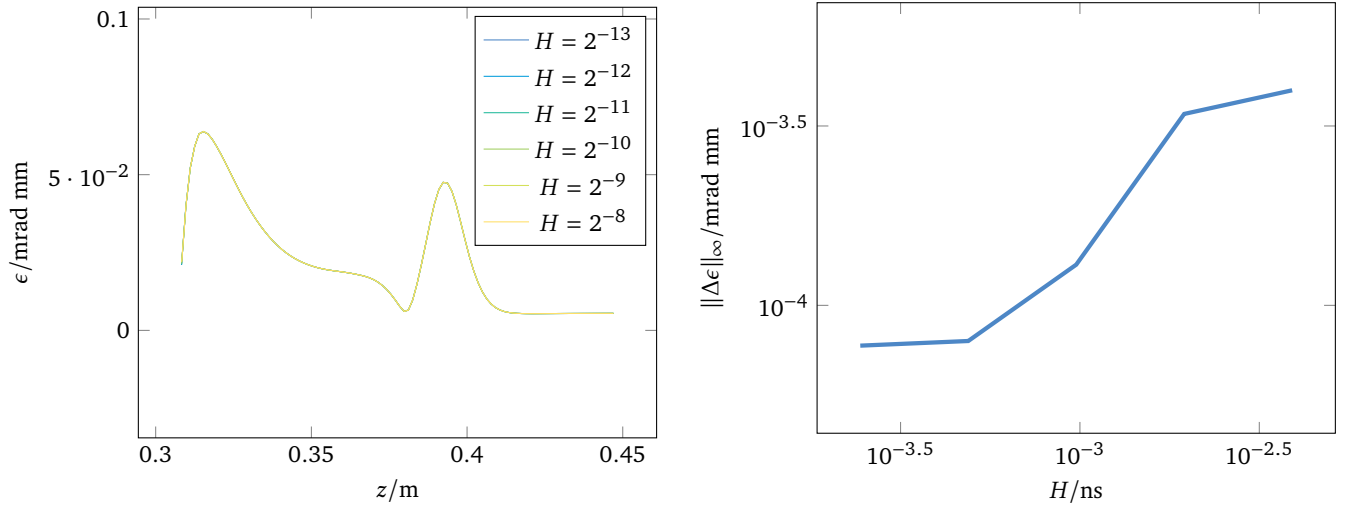


Figure 5: Normalized transverse emittance and absolute error in  $l_{\infty}$ -norm.

- **convergence of field map:** look at convergence with number of grid points in transverse ( $n_x, n_y$ ) and longitudinal ( $n_z$ ) direction individually
- Figure 6 looks at convergence of  $n_x, n_y$  for  $n_z = 64$
- Figure 7 looks at convergence of  $n_z$  for  $n_x = n_y = 16$
- $n_x = n_y = 16$  and  $n_z = 64$  used later on

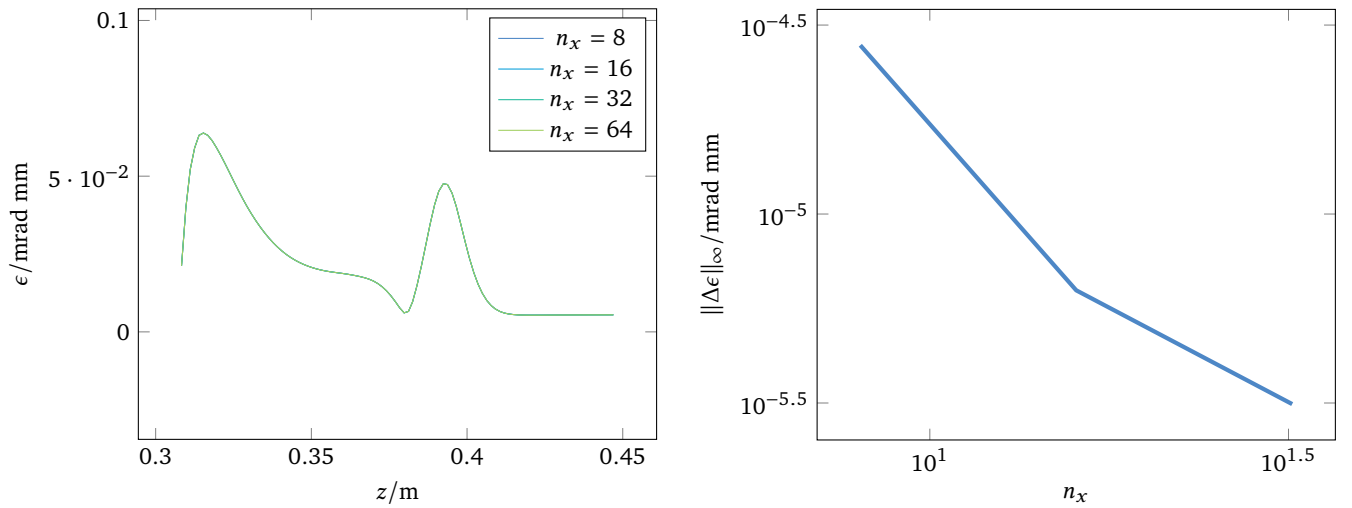


Figure 6: Normalized transverse emittance and absolute error in  $l_{\infty}$ -norm for  $n_z = 64$  and  $n_x = n_y$  variable.

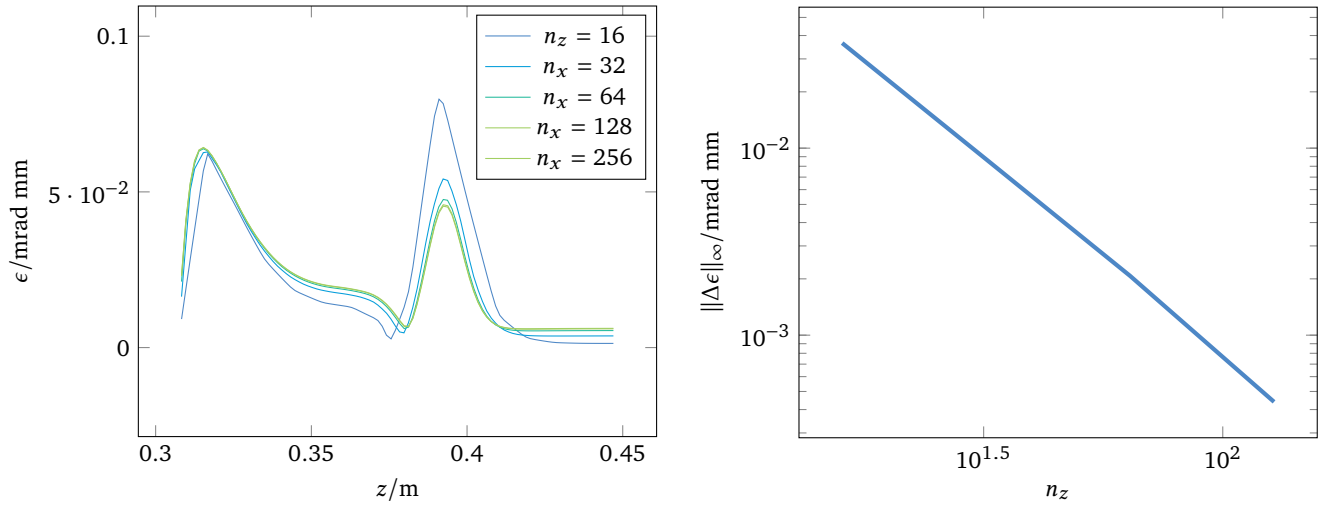


Figure 7: Normalized transverse emittance and absolute error in  $l_\infty$ -norm for  $n_z$  variable and  $n_x = n_y = 16$ .

- **convergence of space charge:** look at convergence with number of grid cells in radial ( $n_r$ ) and longitudinal ( $n_l$ ) direction and number of particles ( $n_I$ ) separately
- Figure 8 looks at convergence of  $n_r, n_l$  for  $n_I = 2^{10}$
- $n_r = n_l = 16$  used later on
- Figure 9 looks at convergence of  $n_I$  for  $n_r = n_l = 16$
- $n_I = 2^{10}$

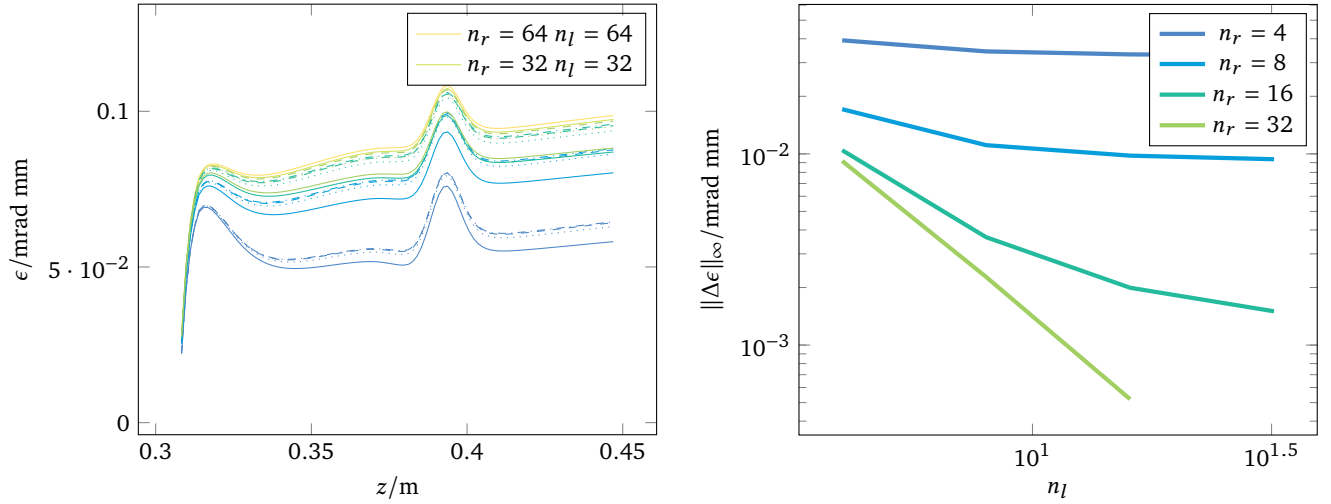


Figure 8: Normalized transverse emittance and absolute error in  $l_\infty$ -norm for  $n_I = 2^{10}$  and  $n_l, n_r$  variable.

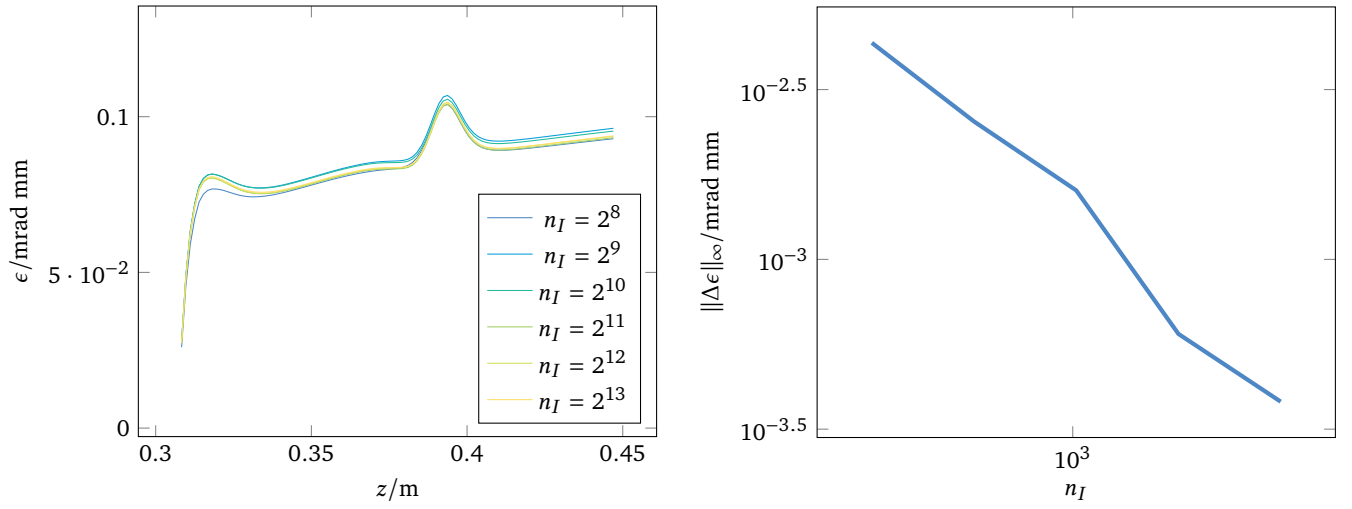


Figure 9: Normalized transverse emittance and absolute error in  $l_\infty$ -norm for  $n_I$  variable and  $n_l = n_r = 16$ .

- **tracking results:**  $\epsilon$  and  $x_{rms}$  computed with the determined settings are shown in Figure 10

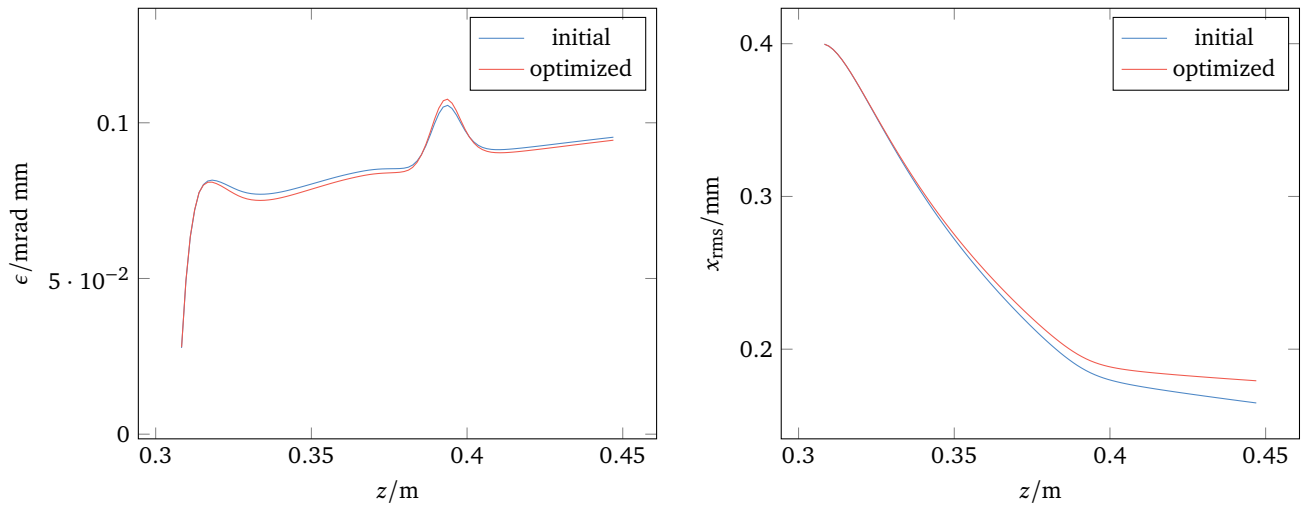


Figure 10: Normalized transverse emittance and rms beam size.

- **remarks:** the convergence studies also looked at  $x_{rms}$  and the behavior was very similar to that of  $\epsilon$
- to minimize the electric field on the entire electrode surface all curves could be taken into account
- this includes the anode ring shape, position and voltage
- also include tracking in optimization via  $x_{rms} \leq 1.5$  mm, also optimize or constrain  $\epsilon \leq 1$  mrad mm?

---

## References

---

- [1] Markus Wagner. “Production and investigation of pulsed electron beams at the S-DALINAC”. PhD thesis. Technische Universität Darmstadt, 2013.